

Experimental Determination of the Mode I Fracture Toughness in Fiber Reinforced Polymer Laminates with Hybrid Delamination Interfaces

Jakub Rzeczkowski^{1*}, Sylwester Samborski², Katarzyna Prokopek³

¹ Department of Technology Fundamentals, Lublin University of Technology, Nadbystrzycka 38, 20-618 Lublin, Poland

² Department of Mechanical Engineering, Lublin University of Technology, Nadbystrzycka 36, 20-618 Lublin, Poland

³ Department of Human Science, Higher School of Economics and Innovation, Projektowa 4, 20-209 Lublin, Poland

* Corresponding author's e-mail: j.rzeczkowski@pollub.pl

ABSTRACT

This paper aims at experimental research of the effect of hybrid interface (carbon/glass fibers) on delamination resistance in unidirectional fiber reinforced polymer (FRP) composite laminates under the mode I opening load conditions. Three group of laminates exhibiting different combinations of reinforcing materials at delamination plane were tested. Critical strain energy release rates were determined by using the double cantilever beam (DCB) tests in accordance with the ASTM D5528 Standard. Values of the G_{IC} were calculated by using classical data reduction schemes and they were compared with values obtained by using an alternative compliance based beam method (CBBM). For precise detection of delamination onset all tests were additionally supported by registration of the acoustic emission (AE) signal. Contribution of mixed-modes were evaluated by using numerical finite element analysis. Obtained outcomes revealed, that differences in the mode I c-SERR values obtained by using four different methods were insignificant. Moreover, the greatest value of the G_{IC} was determined for laminates with hybrid interface and it was equal 0.24 N/mm.

Keywords: DCB tests, hybrid laminates, fracture toughness, composite laminates

INTRODUCTION

Fiber reinforced polymer (FRP) composites are commonly applied in contemporary load-carrying structures. Glass fiber reinforced polymer is incredibly popular reinforcing materials having numerous applications in aircraft or marine industry. Carbon fiber reinforced polymer is extremely strong and enables manufactured of light and thin structures. The price of carbon fiber is generally higher in comparison to the S-glass, such that engineers face a difficult choice between the cost and strength of a structure. Aforementioned problem can be limited by application of hybrid composites that stand out with lower

manufacturing costs with simultaneously maintaining strength parameters.

The composites fabricated of one type of fiber can be called pure composites; on contrary, where more kinds of fibers are used, the hybrid composite is produced. Such composites exhibit good strength at lower cost (compared, for example to pure Kevlar ones) and reveal new fields of material design and applications for engineers [1]. In some laminates, the hybridization has the form of mixing different fibers in the bulk of matrix material [2], whereas in others special sequences of plies are used [3]; texture of the former group is characterized by fiber volume fraction and of the latter – by stacking sequence. Many hybrid

composites have been tested towards their mechanical properties so far. Among the experiments carried out nowadays, four groups of test can be distinguished: tension/compression, flexure, impact, fracture toughness.

Concerning the group of the “bulk” hybrid composites, Fu et al. [4], Xiong et al. [5], Dong [6], Qi et al. [7], Isa et al. [8] showed dependencies of composites’ mechanical properties on fiber type, its volume fraction, as well as orientation angle. Song [9] revealed the difference in mechanical properties comparing different hybrid laminates. Guermazi et al. [10] obtained the mechanical properties of glass-epoxy, carbon-epoxy, and the hybrid of CFRP/GFRP laminates. Joshi et al. [11] analyzed a triple-fiber composite (polypropylene-glass-wollastonite) at various volume fractions, determining the flexure modulus and impact strength.

The layered hybrid composites were tested for flexural, tensile and impact properties by Murugan et al. [12]. The authors considered carbon, glass and hybrid carbon/glass laminates and proved differences in strength among these materials. Randjbaran et al. [13] examined hybrid carbon, glass and kevlar fibers for impact and proved that the stacking sequence influenced the energy absorption. Also Yang et al. [14] prepared impact tests on the CFRP/GFRP hybrids at different velocities of the projectile; the pure composite absorbed less energy than the hybrid laminates. As shown by Jalavand et al. [15], the free edges effects can be observed during delamination of hybrid directional composites, which is in contrary to damage modes observed in the UD hybrid laminates. Mechanical properties and damage mechanisms in hybrid laminates including organic reinforcement (flax) [16,17] were examined, as well – in tension and three-point bending (3PB); in addition damage phenomena were monitored and detected with the so-called acoustic emission (AE) technique. For flax-glass specimens different damage mechanism at the interface was observed.

The objectives of this study was to investigate the effect of hybrid interface on delamination resistance in FRP laminates with respect to

the composites with monomaterial reinforcement in layers at delamination plane. Mode I c-SERR was determined by using the DCB tests supported by the acoustic emission technique.

EXPERIMENTAL PROCEDURE

Experimental determination of the mode I delamination resistance values were prepared on unidirectional $[0^0_{16}]$ fiber reinforced polymer (FRP) composite laminates with combination of different reinforcing materials (glass fiber reinforced polymer GFRP and carbon fiber reinforced polymer CFRP) in layers at delamination plane. In general, the comparison of fracture properties were performed for three groups of laminates with various material compositions at delamination interfaces, namely: CFRP//CFRP, GFRP//GFRP and hybrid CFRP//GFRP (note that “//” stands for delamination plane). In the context of current paper, the term “hybrid” applies to a combination of the glass fiber and carbon fiber layers laminated together. Particular description of tested specimens were presented below. The green color refers to the carbon/epoxy and red color refers to the glass/epoxy laminas.

- DCB 1 – $[0^0_7 0^0//0^0/0^0_7]$ CFRP//CFRP
- DCB 2 – $[0^0_7 0^0//0^0/0^0_7]$ GFRP//GFRP
- HYB – $[0^0_7 0^0//0^0/0^0_7]$ hybrid GFRP//CFRP

Material properties of the CFRP and the GFRP materials were determined during tensile tests and obtained material properties were collected in the Table 1 and Table 2.

All experiments were prepared by using the double cantilever beam (DCB) tests according to the ASTM D5528 Standard regulations [18]. The main dimensions of laminate beam specimens were: total length $L = 150$ mm, total thickness $2h = 2.1$ mm and width $B = 25$ mm. A thin teflon foil was placed at the mid-plane of laminate beams and served as delamination starter – initial delamination length was equal $a_0 = 30$ mm. Experimental tests were performed on the Shimadzu ASG-X tensile testing machine with constant traverse

Table 1. Material constants of carbon/epoxy obtained during tensile test

E_1 [GPa]	E_2 [GPa]	ν_{12} [-]	G [GPa]
148.051	5.330	0.312	3.968

Table 2. Material constants of glass/epoxy obtained during tensile test

E_1 [GPa]	E_2 [GPa]	ν_{12} [-]	G [GPa]
34.699	16.818	0.167	4.189

velocity 1 mm/min. During the DCB experiments, applied displacement (δ) and resultant load (P) were registered. In addition, all crack tip propagation values were marked on both edges of specimens. In order to increase a precise determination of delamination onset the acoustic emission (AE) technique was used. A piezoelectric sensor was bonded at one end of specimen and registered in real time various parameters of AE waves. Delamination initiation point was adopted as a first rapid growth of cumulative energy of acoustic emission signal. Typical DCB experimental setup was presented in Figure 1.

Mode I fracture toughness, represented by the critical strain energy release rate (c-SERR, G_{IC}) were calculated by using different methods recommended in the ASTM Standard: the modified beam theory (MBT), the compliance calibration method (CCM) and the modified compliance calibration (MCC). Moreover, the mode I c-SERR values were calculated by using the alternative compliance based beam method (CBBM) elaborated by de Moura [19]. The main advantages of this method is that it does not require visual observation of crack tip and it takes into account a fracture process zone developing ahead of the crack front. Data reduction schemes for determination of the G_{IC} by using the MBT, CCM, MCC and CBBM methods are represented by equations 1-4 respectively:

$$G_{IC} = \frac{3P\delta}{2B(a+|\Delta|)} \quad (1)$$

$$G_{IC} = \frac{nP\delta}{2aB} \quad (2)$$

$$G_{IC} = \frac{3P^2C^{2/3}}{2A_1Bh} \quad (3)$$

$$G_{IC} = \frac{12P^2a_e^2}{B^2h^3E_f} \quad (4)$$

where: C is laminate compliance,
 E_f is flexural modulus and
 A_1, n, Δ are correction parameters.

In order to distinguish contributions of different fracture modes, an analytical approach [20] was considered, besides finite element simulations. Numerical analysis were conducted in Abaqus/CAE software environment by using the virtual crack closure technique VCCT. The formula that was used to express a prediction of delamination growth was Reeder Low criterion, that take into account the mixed-modes effect. The

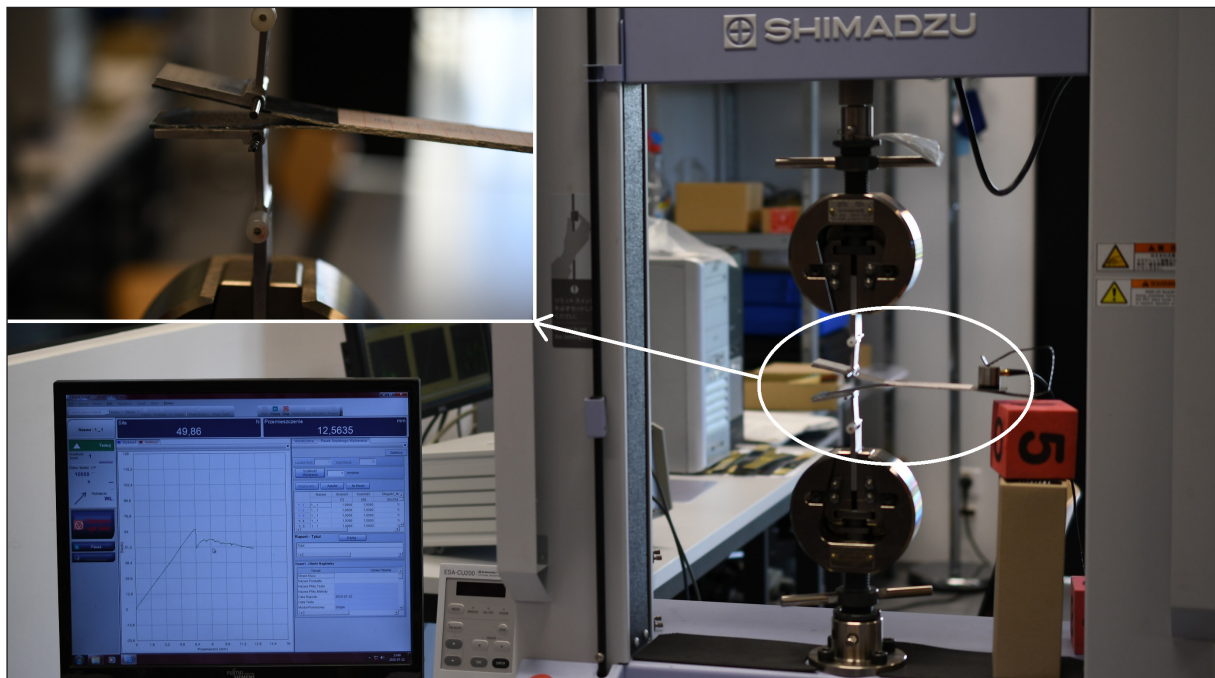


Fig. 1. Experimental DCB test setup

mesh of beam model consisted of 11 400 S4 and S4R shell elements.

RESULTS AND DISCUSSIONS

The mode I c-SERRs were determined for three groups of laminates with different reinforcing materials at delamination interfaces. Obtained values of the mode I c-SERR calculated by using various data reduction schemes, for three specimens in each group, were collected in the Table 3. The average values of the G_{IC} were presented in the Table 4.

Considering average values of the mode I c-SERR, it can be observed, that differences between G_{IC} determined by using classical methods recommended in the ASTM Standard were insignificant for each laminate’s configuration. In practice, the most recommended methods is the modified beam theory, due to it takes into account a displacement in its data reduction schemes. The critical strain energy release rate calculated by using the alternative compliance based beam method were in similar level in comparison to values obtained by using standard methods. It proved, that the fracture process zone in case of the unidirectional laminates is small, and can be neglected during determination of the total delamination resistance under opening mode I loading. Comparing laminates with carbon//carbon and glass//glass fiber delamination interfaces, a value of the G_{IC} was about 0.10 N/mm for the DCB 1 configuration, whereas for the DCB 2 specimen, those values reached around 0.13 N/mm. The greatest values of the mode I critical strain energy release rate exhibited laminates with hybrid interface. For this case, the mode I c-SERR was equal on average level 0.22 N/mm. Increased in the critical strain energy release rate values for laminate with hybrid (GFRP/CFRP) interface could be physically clarified as a results of synergy between

carbon/epoxy and glass/epoxy stiffness that requires more energy to propagate the crack, thus higher values of the G_{IC} were obtained. In addition, the hybrid fiber bridging phenomenon and rougher fracture surface, as well as the little contribution from fracture mode II (due to asymmetric stacking sequence) could also influence the greater values of c-SERR, in comparison to pure glass fiber or pure carbon fiber interfaces.

Typical load-cumulative energy versus time plots obtained during experimental tests for different types of laminates were presented in Figures 2, 3, 4. The end of vertical solid lines marked on diagrams indicate the AE criteria that correspond to initiation of delamination point. It should be emphasized, that for all cases, sudden growth of cumulative energy appeared before the peak force on load-time plots. It was in agreement with the *NL* approach according to the ASTM recommendations, which is not easy to define experimentally. On the other hand, it was an evidence, that delamination started to propagate inside the material without any visible cracks on specimen edges. Therefore, the AE technique was successfully utilized to increase the precise detection of delamination onset with simultaneously reducing errors during experimental determination of the fracture toughness. Regarding to composites with glass/epoxy and hybrid delamination planes, although small differences in load versus time trends could be observed, the cumulative energy plots overlapped itself for all cases. In addition, slight irregularities on *P*-time plots can be related with effect of bridging failure mechanism.

The mode I strain energy release rate width-wise distributions (mode I SERR) plots obtained during the finite element numerical analysis were presented in Figure 5. It can be observed, that all diagrams were symmetric with respect to the beam model center, where for all laminates, the mode I SERR reached the greatest values; they were as follows: $G_I=0.11$ N/mm for DCB-1 and DCB-2

Table 3. Values of the mode I c-SERR determined for composite laminates with various delamination interfaces calculated by using classical and alternative calculation methods for three specimens in each laminate’s configuration

Specimen no.	Mode I c-SERR [N/mm]											
	[01]				[02]				[03]			
Configuration	CCM	MBT	MCC	CBBM	CCM	MBT	MCC	CBBM	CCM	MBT	MCC	CBBM
DCB 1	0.09	0.08	0.10	0.09	0.09	0.08	0.09	0.08	0.11	0.11	0.12	0.13
DCB 2	0.14	0.14	0.16	0.15	0.12	0.12	0.12	0.13	0.12	0.11	0.17	0.11
HYB	0.25	0.22	0.25	0.23	0.24	0.24	0.24	0.25	0.19	0.18	0.22	0.19

Table 4. Average values of the mode I c-SERR determined for laminates with different delamination interfaces calculated by using classical and alternative calculation methods

Average values of the mode I c-SERR [N/mm]				
Configuration	CCM	MBT	MCC	CBBM
DCB 1	0.09	0.09	0.10	0.10
DCB 2	0.13	0.12	0.15	0.13
HYB	0.23	0.21	0.24	0.22

specimens and $G_I=0,2$ N/mm for laminate with hybrid interface. Fracture modes II and III were on average around 1×10^{-27} N/mm, hence they were not presented on the SERR distribution plots. Nevertheless, for HYB specimens, the analytical model by Valvo [20] furnished a contribution of the sliding mode, $G_{II}/G = 2.6\%$, which is small but not negligible. Although the values of the mode II and mode III SERR were minimal in comparison to the mode I SERR, the sliding and tearing modes could influence the greater fracture toughness values obtained in case of the hybrid laminates.

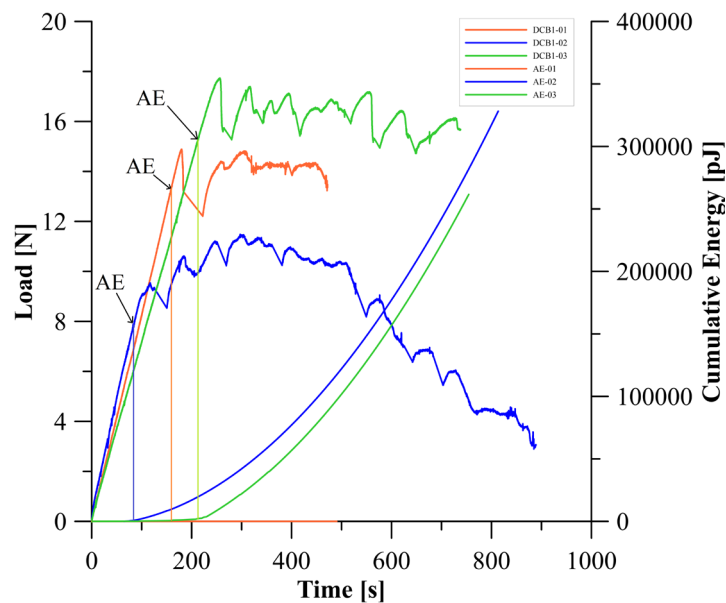


Fig. 2. Specific load-cumulative energy versus time plots for composite laminates with carbon// carbon fibers delamination interfaces obtained during the double cantilever beam experiments

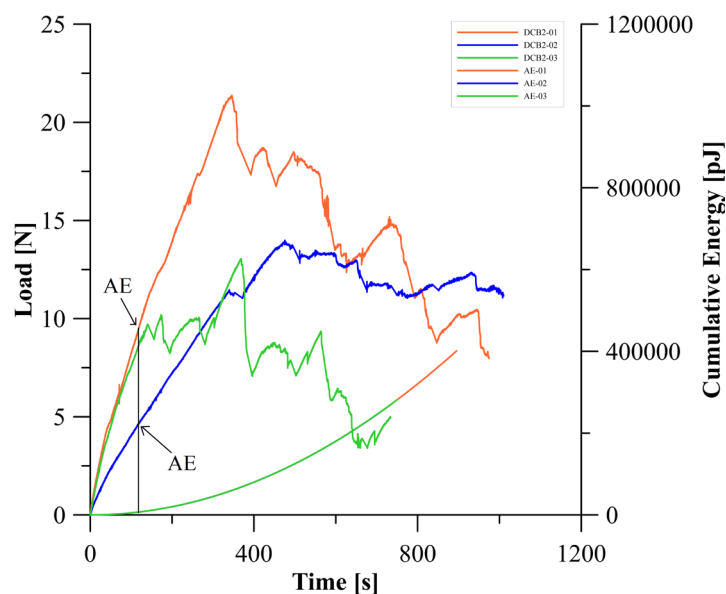


Fig. 3. Specific load-cumulative energy versus time plots for composite laminates with glass// glass fibers delamination interfaces obtained during the double cantilever beam experiments

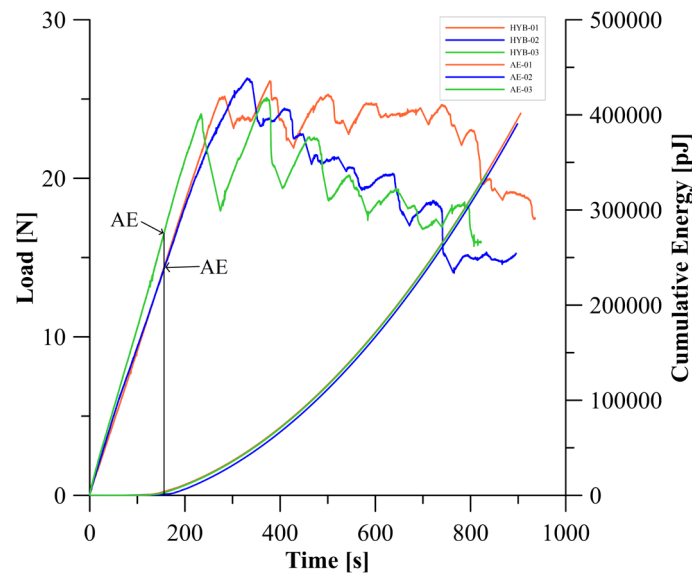


Fig. 4. Specific load-cumulative energy versus time plots for composite laminates with hybrid delamination interfaces obtained during the double cantilever beam experiments

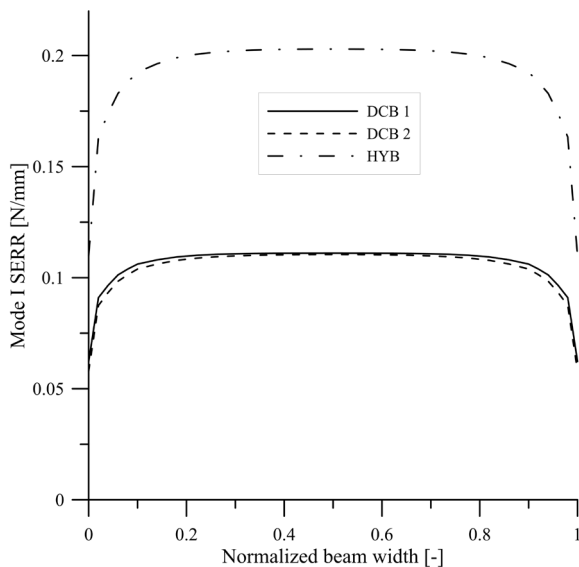


Fig. 5. Mode I SERR widthwise distributions for different DCB composite laminates beams

Obtained outcomes revealed, that differences in the mode I c-SERR values obtained by using different methods were insignificant. The greatest value of the critical SERR was obtained for laminate with hybrid delamination interface and it was equal 0.24 N/mm. Increased in the G_{IC} values, in compared to the glass/epoxy and carbon/epoxy interfaces, could physically be explained by synergy between CFRP and GFRP stiffness, fiber bridging phenomena, as well as contribution of mixed-modes. Applicability of the acoustic emission technique allowed to increase the precise detection of delamination onset. The first rapid growth in cumulative counts indicated initiation of delamination. In addition, the AE point correspond to the NL criteria recommended by the ASTM Standard.

CONCLUSIONS

In this article, the effect of hybrid delamination interface in unidirectional FRP laminates on fracture toughness was characterized. Laminates with different combination of reinforcing materials (carbon//carbon, glass//glass and hybrid glass/carbon) at delamination plane were investigated under the double cantilever beam tests prepared in accordance with the ASTM D5528 Standard. The mode I critical strain energy release rates were determined by using classical data reduction schemes, as well as by using the alternative compliance based beam method.

REFERENCES

1. Rakesh P, Diwakar V, Venkatesh K, Savannanavar RN. A Concise Report on properties of Hybrid Composites manufactured from glass and natural fibers. *Materials Today: Proceedings* 2020;22(2):2008–15.
2. Almansour FA, Dhakal HN, Zhang ZY. Investigation into Mode II interlaminar fracture toughness characteristics of flax/basalt reinforced vinyl ester hybrid composites. *Composites Science and Technology* 2018;154(25):117–27.
3. Hung P-y, Lau K-t, Cheng L-k, Leng J, Hui D. Impact response of hybrid carbon/glass fibre reinforced polymer composites designed for engineer-

- ing applications. *Composites Part B: Engineering* 2018;133:86–90.
4. Fu Y, Zhang P, Yang F. Interlaminar stress distribution of composite laminated plates with functionally graded fiber volume fraction. *Materials & Design* 2010;31(6):2904–15.
 5. Xiong W, Blackman B, Dear JP, Wang X. The effect of composite orientation on the mechanical properties of hybrid joints strengthened by surf-sculpt. *Composite Structures* 2015;134(4):587–92.
 6. Dong C, Davies IJ. Flexural strength of bidirectional hybrid epoxy composites reinforced by E glass and T700S carbon fibres. *Composites Part B: Engineering* 2015;72(1):65–71.
 7. Qi LH, Ma YQ, Zhou JM, Hou XH, Li HJ. Effect of fiber orientation on mechanical properties of 2D-C f /Al composites by liquid–solid extrusion following Vacuum infiltration technique. *Materials Science and Engineering: A* 2015;625:343–9.
 8. Isa MT, Ahmed AS, Aderemi BO, Taib RM, Mohammed-Dabo IA. Effect of fiber type and combinations on the mechanical, physical and thermal stability properties of polyester hybrid composites. *Composites Part B: Engineering* 2013;52(4):217–23.
 9. Song JH. Pairing effect and tensile properties of laminated high-performance hybrid composites prepared using carbon/glass and carbon/aramid fibers. *Composites Part B: Engineering* 2015;79(5):61–6.
 10. Guermazi N, Haddar N, Elleuch K, Ayedi HF. Investigations on the fabrication and the characterization of glass/epoxy, carbon/epoxy and hybrid composites used in the reinforcement and the repair of aeronautic structures. *Materials & Design* 2014;56:714–24.
 11. Himani J, Purnima J. Development of glass fiber, wollastonite reinforced polypropylene hybrid composite: Mechanical properties and morphology. *Materials Science and Engineering: A* 2010;527(7-8):1946–51.
 12. Murugan R, Ramesh R, Padmanabhan K. Investigation on Static and Dynamic Mechanical Properties of Epoxy Based Woven Fabric Glass/Carbon Hybrid Composite Laminates. *Procedia Engineering* 2014;97(1):459–68.
 13. Randjbaran E, Zahari R, Jalil NAA, Majid DLAA. Hybrid composite laminates reinforced with Kevlar/carbon/glass woven fabrics for ballistic impact testing. *ScientificWorldJournal* 2014;2014:413753.
 14. Yang B, Wang Z, Zhou L, Zhang J, Liang W. Experimental and numerical investigation of interply hybrid composites based on woven fabrics and PCBT resin subjected to low-velocity impact. *Composite Structures* 2015;132:464–76.
 15. Fotouhi M, Jalalvand M, Wisnom MR. Notch insensitive orientation-dispersed pseudo-ductile thin-ply carbon/glass hybrid laminates. *Composites Part A: Applied Science and Manufacturing* 2018; 110(14): 29–44.
 16. Audibert C, Andreani A-S, Lainé É, Grandidier J-C. Mechanical characterization and damage mechanism of a new flax-Kevlar hybrid/epoxy composite. *Composite Structures* 2018;195(9):126–35.
 17. Saidane EH, Scida D, Assarar M, Ayad R. Damage mechanisms assessment of hybrid flax-glass fibre composites using acoustic emission. *Composite Structures* 2017;174(11):1–11.
 18. D30 Committee. Test Method for Mode I Interlaminar Fracture Toughness of Unidirectional Fiber-Reinforced Polymer Matrix Composites. West Conshohocken, PA: ASTM International; 2013. doi:10.1520/D5528-13.
 19. Rzeczkowski J, Samborski S, Moura M de. Experimental Investigation of Delamination in Composite Continuous Fiber-Reinforced Plastic Laminates with Elastic Couplings. *Materials (Basel)* 2020;13(22).
 20. Valvo PS. On the calculation of energy release rate and mode mixity in delaminated laminated beams. *Engineering Fracture Mechanics* 2016;165:114–39.